Innate Immune-Directed NF-κB Signaling Requires Site-Specific NEMO Ubiquitination

Janice C. Jun,[1,2] Sylvia Kertesy,[1,2] Mark B. Jones,[1] Jill M. Marinis,[1,3] Brian A. Cobb,[1] Justine T. Tigno-Aranjuez,[1] and Derek W. Abbott[1,*]

[1]Department of Pathology, Case Western Reserve School of Medicine, Cleveland, OH 44106, USA
[2]These authors contributed equally to this work and are listed alphabetically
[3]Present address: Division of Endocrinology, Diabetes, and Metabolism, Perelman School of Medicine, University of Pennsylvania, Philadelphia, PA 19104, USA
*Correspondence: dwa4@case.edu
http://dx.doi.org/10.1016/j.celrep.2013.06.036

SUMMARY

While the I kappa kinase (IKK) scaffolding protein NF-κB essential modulator (NEMO) binds to polyubiquitin chains to transmit inflammatory signals, NEMO itself is also ubiquitinated in response to a variety of inflammatory agonists. Although there have been hints that polyubiquitination of NEMO is essential for avoiding inflammatory disorders, the in vivo physiologic role of NEMO ubiquitination is unknown. In this work, we knock in a *NEMO* allele in which two major inflammatory agonist-induced ubiquitination sites cannot be ubiquitinated. We show that mice with a nonubiquitinatable *NEMO* allele display embryonic lethality. Heterozygous females develop inflammatory skin lesions, decreased B cell numbers, and hypercellular spleens. Embryonic lethality can be complemented by mating onto a *TNFR1*^{−/−} background, at the cost of severe steatohepatitis and early mortality, and we also show that NEMO ubiquitination is required for optimal innate immune signaling responses. These findings suggest that NEMO ubiquitination is crucial for NF-κB activity in response to innate immune agonists.

INTRODUCTION

Nontraditional ubiquitination plays a critical role in innate immune signaling, and in no innate immune signaling pathway is this better described than in the NF-κB pathway. In response to a variety of inflammatory agonists, E3 ubiquitin ligases such as TRAF2, TRAF6, cIAP1/2, and LUBAC are activated and induce both K63-linked and linear ubiquitination of key signaling proteins such as RIP1, RIP2, TAK1, and NF-κB essential modulator (NEMO). These polyubiquitin chains then serve as binding surfaces to link signal transduction proteins and initiate and sustain an NF-κB response. This theme is repeated across multiple signaling pathways that culminate in NF-κB activation, including

the tumor necrosis factor (TNF), Toll-like receptor (TLR), and nucleotide oligomerization domain (NOD) signaling pathways, and is required for physiologic inflammation and the avoidance of autoinflammatory disease (all reviewed in Chen, 2012, and Hayden and Ghosh, 2012). Ultimately, these ubiquitin signaling cascades converge upon the I kappa kinase (IKK) signalosome, which in its most rudimentary form consists of IKKα and IKKβ both bound to the scaffolding protein NEMO. Within this central NF-κB signaling hub, NEMO binds ubiquitin directly. It binds both lysine 63 (K63)-linked and linear ubiquitin chains to allow activation of the IKKs and NF-κB nuclear translocation with subsequent gene expression (Wu et al., 2006; Cordier et al., 2009; Laplantine et al., 2009; Lo et al., 2009; Rahighi et al., 2009, Hadian et al., 2011; Ikeda et al., 2011; Kensche et al., 2012).

Lost in the fact that NEMO's ubiquitin binding is a central feature of inflammatory signal coordination is that NEMO itself is both K63 and linearly polyubiquitinated (Abbott et al., 2004, Zhou et al., 2004, Tokunaga et al., 2009). In a prominent, disease-related example, activation of the Crohn's disease susceptibility protein, NOD2, causes ubiquitination of NEMO at lysine 285 (K285). Loss-of-function Crohn's-disease-associated polymorphisms do not allow this ubiquitination to occur, and this loss of ubiquitination correlates with a substantial decrease in NF-κB signaling in response to NOD2 activation (Abbott et al., 2004, 2007; reviewed in Chen et al., 2009). While NOD2 allows recognition of intracellular bacterial invasion by sensing a breakdown product of peptidoglycan called muramyl dipeptide (MDP) (Girardin et al., 2003; Inohara et al., 2003), extracellular innate immune sensors also require NEMO ubiquitination for signaling. Lipopolysaccharide (LPS) induces ubiquitination of NEMO at a site presumed to be K399, and if this major LPS-induced NEMO ubiquitination site is mutated in vivo, mice fail to achieve a productive cytokine response and become hyperresistant in LPS-sepsis models (Ni et al., 2008). Thus, although NEMO's ubiquitin-binding capabilities have received much more attention, its own ubiquitination appears to be equally important for optimal NF-κB signaling in response to inflammatory agonists.

Like K399 ubiquitination on NEMO, NEMO ubiquitination at K285 also appears to be crucial for innate immune responses

(Abbott et al., 2004; Belgnaoui et al., 2012; Hinz et al., 2010; Kim et al., 2011; Niu et al., 2011). It is required for effective viral responses in tissue culture systems (Zhao et al., 2007; Belgnaoui et al., 2012), and work in our laboratory has shown that in both tissue culture and reconstitution systems, K285 ubiquitination is crucial for NOD2 signaling (Abbott et al., 2004, 2007). To date, though, although a major innate immune ubiquitination site (mouse K392, human K399) has been mutated in the whole mouse (Ni et al., 2008), the other major innate immune ubiquitination site, K285, has not been mutated in vivo. Although K285 ubiquitination is crucial for NOD2 signaling in vitro and is thus suggested to be important in pathophysiologic disease states in which NOD2 signaling is dysregulated, its role in NOD2 signaling in nonoverexpression/reconstitution systems remains speculative. The physiologic effect of this key NEMO ubiquitination site is unknown, and the consequence of the combined lack of ubiquitination of these two major innate immune ubiquitination sites is unknown.

Given the questions surrounding NEMO ubiquitination, we generated a mouse that contained a humanized NEMO complementary DNA (cDNA) with K285 and K399 mutated to arginines. In previous tissue culture studies, we found that NEMO with this K285RK399R mutation could bind to the IKKs normally, but could not signal properly in reconstituted MEF experiments (Abbott et al., 2007). In the current in vivo study, we found that the lack of ubiquitination on K285 and K399 caused embryonic lethality in mice. Heterozygous knockin mice developed severe skin ulcerations and inflammation that correlated with enlarged spleens, decreased splenic B cells, and increased splenic $Gr_1^+CD11_b^+$ cells. This embryonic lethality and inflammatory phenotype can be genetically complemented by mating these mice with TNFR1$^{-/-}$ null mice, suggesting a genetic interaction between the TNF pathway and NEMO ubiquitination. Despite the fact that nonubiquitinatable NEMO no longer caused embryonic lethality, the TNFR1$^{-/-}$X^{NemoKi}Y mice showed increased mortality and evidence of severe steatohepatitis. Lastly, the TNFR1$^{-/-}$X^{NemoKi}Y mice were severely defective in NOD2, TLR4, and interleukin-1 (IL-1) signaling, suggesting that ubiquitination of NEMO is essential for optimal innate immune-induced cytokine production. In sum, this work provides evidence that ubiquitination of NEMO is essential for proper functioning of the NF-κB pathway, as the lack of ubiquitinated NEMO largely phenocopies NEMO null mice. It also provides evidence of complementarity of TNF signaling with NEMO ubiquitination and establishes the in vivo role of NEMO ubiquitination in innate immune signaling. Thus, while NEMO has received much attention for its role as a ubiquitin-binding protein, its own ubiquitination is also crucial for NF-κB function.

RESULTS

To determine the in vivo role of two major innate immune NEMO ubiquitination sites, we generated a targeting construct that contained a myc-tagged human NEMO cDNA containing lysines 285 and 399 mutated to arginine. In our previous studies we found that this N-terminally myc-tagged mutant NEMO bound the IKKs identically to untagged NEMO, and myc-tagged wild-type (WT) NEMO was able to reconstitute NF-κB signaling in NEMO

null MEFs identically to untagged NEMO (Abbott et al., 2004, 2007). This cDNA was knocked into the endogenous NEMO locus on the X chromosome such that it replaced exons 2–5 (Figure 1A). After establishing germline transmission, we mated the NEMO knockin mice with flippase (FLP) recombinase mice to remove the NEO cassette, and then backcrossed them ten times onto C57BL/6 to establish the X^{WT}X^{NemoKi} line. Evidence of protein expression (both with NEMO antibodies and via the myc tag) and germline transmission is shown in Figure 1B. Matings aimed at generating male NEMO knockin mice showed that, even though >200 mice were generated, none were X^{NemoKi}Y suggesting embryonic lethality (Figure 1C). The female heterozygous mice displayed difficult fecundacy, as times between litters varied between 27 and 90 days and did not display consistency within a single mother or across mothers.

In addition to fertility difficulties, female heterozygous mice developed ulcerating skin lesions (Figure 2A). Histologically, these lesions showed hyperkeratosis and parakeratosis with elongated rete ridges (Figure 2A) suggestive of a psoriasis-like histology. Quantitative RT-PCR (qRT-PCR) analysis of lesional skin showed elevated cytokines in the heterozygous NEMO knockin mice compared with WT littermate controls (Figure 2B). This skin inflammation correlated with the appearance of a greatly enlarged spleen (Figure 2C). Quantitatively, the splenic enlargement was due to an abundance of Gr1$^+$CD11b$^+$ cells (Figure 2C), suggesting an inflammatory phenotype in these mice. Splenic T cell counts were similar between WT and heterozygous NEMO knockin mice, whereas splenic B cells were decreased in the NEMO knockin mice (Figure 3). These findings are consistent with the requirement for functional NEMO in B cell development (Kim et al., 2003; Derudder et al., 2009). The results obtained in the heterozygous NEMO knockin female mice closely resemble those obtained in the heterozygous NEMO knockout female mice. These heterozygous complete knockout mice develop alopecia and inflammatory skin lesions, albeit in a much more severe manner and at a much earlier age (Makris et al., 2000; Rudolph et al., 2000; Schmidt-Supprian et al., 2000). This fact, coupled with the embryonic lethality seen with both a null allele and the K285RK399R allele, suggests that the K285RK399R NEMO knockin allele is a loss-of-function allele, and that after the loss of these two ubiquitination sites, it resembles a null NEMO allele.

Due to the reproductive difficulties in the heterozygous NEMO knockin mice, and because X inactivation essentially causes chimerism in the heterozygous NEMO knockin mice, instead of performing timed matings in a line with extremely irregular estrous and birth cycles, we took an alternative approach to determine the cause of embryonic lethality. NEMO null mice die at E12–E13 because of massive liver apoptosis due to an imbalance in TNF signaling favoring JNK-mediated apoptosis over NF-κB-induced survival (Makris et al., 2000; Rudolph et al., 2000; Schmidt-Supprian et al., 2000). Therefore, we sought to determine whether TNF receptor (TNFR) loss would complement the embryonic lethality in the NEMO knockin mice. To this end, we mated TNFR1$^{-/-}$ mice to the TNFR1$^{-/-}$ heterozygous NEMO knockin mice to generate TNFR1$^{-/-}$ X^{NemoKi}Y mice. Although these mice were generated at less-than-Mendelian ratios, TNFR1$^{-/-}$X^{NemoKi}Y were viable,
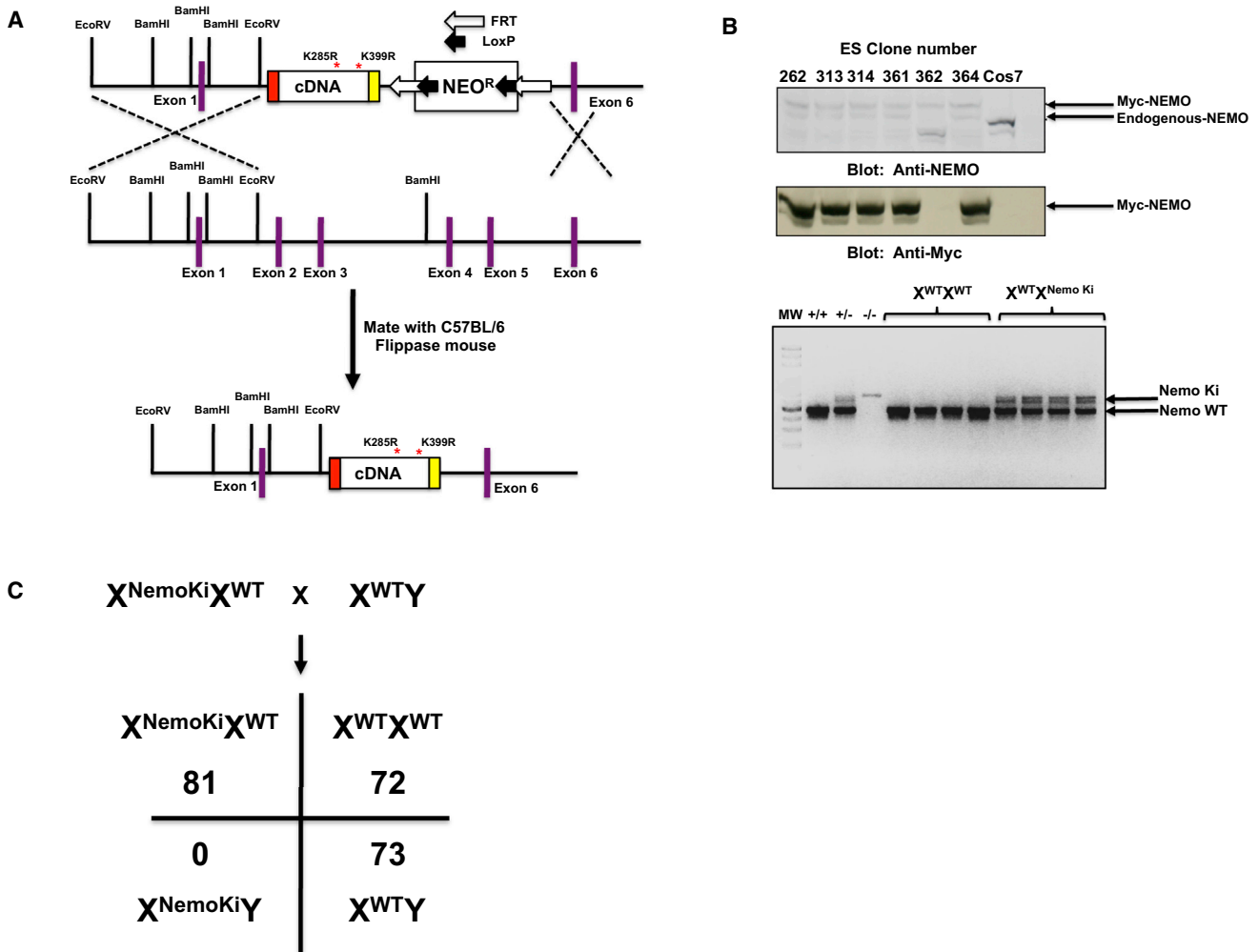
Figure 1. Knockin of a Nonubiquitinatable NEMO Allele Causes Embryonic Lethality

(A) Schematic of the targeting construct used to generate a nonubiquitinatable NEMO mouse. Exons 2–5 were replaced with a cDNA encoding NEMO in which lysines 285 and 399 were replaced with arginines such that ubiquitination could not occur. The construct was tagged on the N terminus with a myc tag such that it could be differentiated from endogenous NEMO. Additionally, the NEO cassette was flanked by FRT sites such that when it was generated, the mouse could be mated with a Flippase mouse to remove the NEO cassette.

(B) Stably transfected ES clones were assayed for nonubiquitinatable NEMO expression. An anti-myc western blot showed expression of the nonubiquitinatable myc gene, and an anti-NEMO blot showed relative expression of endogenous knocked-in NEMO in the ESCs (upper panels). The lower panel shows germline transmission in heterozygous female mice.

(C) Mendelian ratios of matings of WT male BL/6 mice with heterozygous female NEMO knockin mice. NEMO is on the X chromosome, and no NEMO knockin males were observed in the >200 mice generated.

suggesting that TNFR1 loss can complement the nonubiquitinatable NEMO phenotype (Figure 4A). Both the skin lesions and hypercellularity of the spleens were not present in the TNFR$^{-/-}$X^{NemoKi}Y mice, further suggesting that TNF signaling is responsible for the skin inflammation in the X^{WT}X^{NemoKi} mice, and consistent with the results showing that the skin defect in NEMO null mice can be reversed by mating onto a TNFR1 null background (Nenci et al., 2006). The TNFR1$^{-/-}$X^{NemoKi}Y were not entirely healthy, however, as they showed increased mortality relative to either WT or TNFR1$^{-/-}$ mice (Figure 4B). Whole necropsy showed normal development and histology of organs, with the exception of a substantially diseased liver. Histologi-

cally, the liver showed evidence of macro- and microvesicular steatosis with centrilobular and zone 3 hepatitis, moderate fibrosis, and regenerative nodules (Figure 4C). Hepatocytes showed dysplasia with prominent nucleolar vacuoles (Figure 4C). Liver function tests showed greatly elevated aspartate transferase (AST), alanine transferase (ALT), lactate dehydrogenase (LDH), and total bilirubin, suggesting hepatocyte cell death and acute hepatitis (Figure 4D). Together, these features closely resemble those of nonalcoholic steatohepatitis (NASH) and the phenotype of the hepatocyte-specific NEMO knockout mouse (Beraza et al., 2007, 2009; Luedde et al., 2007), again suggesting that the nonubiquitinatable NEMO is a loss-of-function allele.
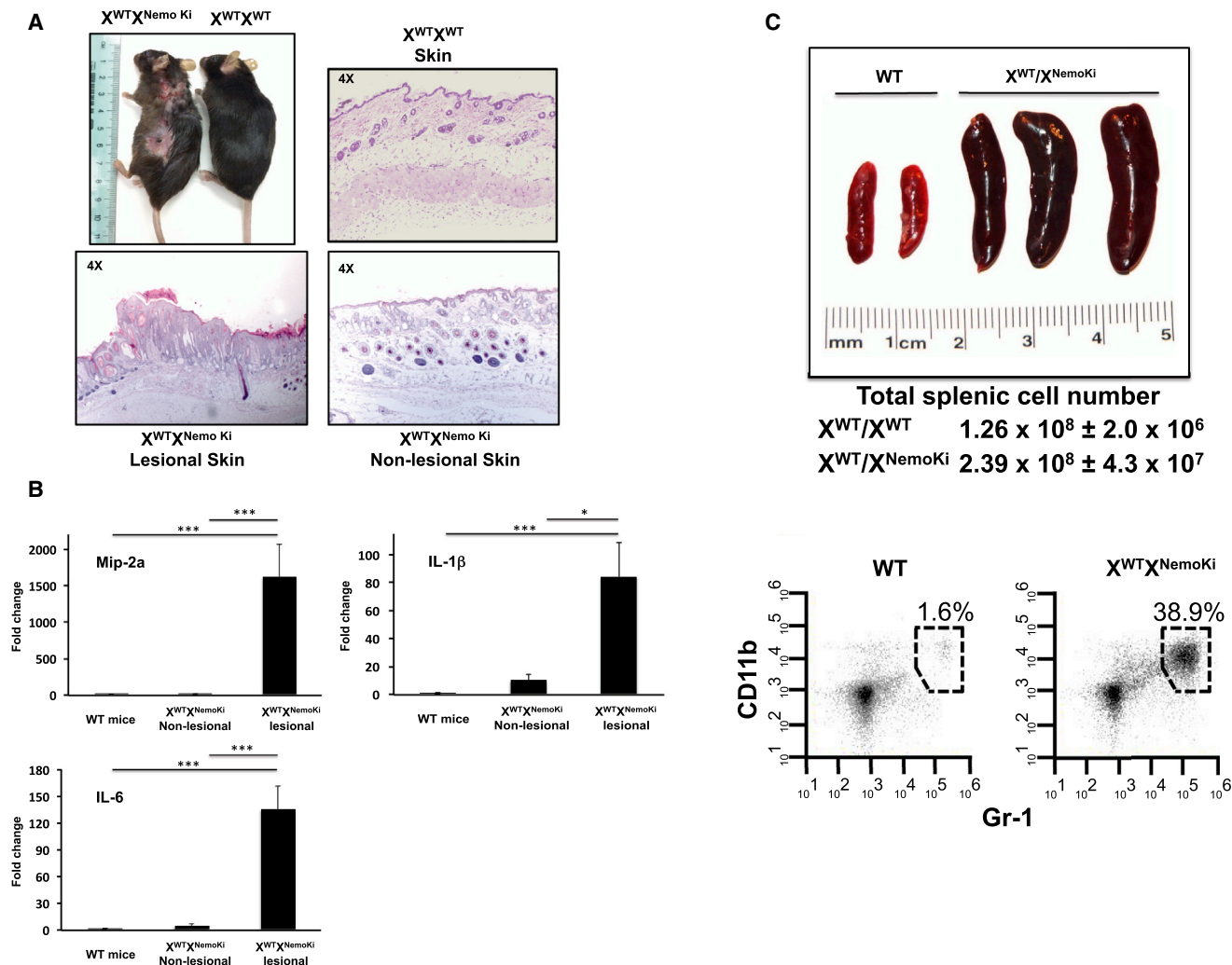
Figure 2. Nonubiquitinatable NEMO Knockin Mice Develop Inflammatory Skin Lesions and Splenomegaly

(A) Gross photograph of a representative 8-month-old nonubiquitinatable NEMO heterozygous female compared with a WT mouse. The nonubiquitinatable NEMO heterozygous mice develop ulcerated and plaque-like lesions distributed throughout the body. Histologically, the plaque-like skin lesions show hyper-keratosis, parakeratosis, keratin pearls, and a hyperproliferative epidermis with rete-ridge-like protrusions into the dermis. Nonlesional skin from the non-ubiquitinatable heterozygous NEMO knockin mice shows little histological change relative to WT mice.

(B) qRT-PCR analysis of cytokines from the skin of WT littermates or from lesional or nonlesional skin from heterozygote nonubiquitinatable NEMO knockin mice (n = 3). Cytokines are significantly elevated in both the lesional and nonlesional skin from the nonubiquitinatable NEMO heterozygous mice. SEM, *p < 0.05, ***p < 0.001.

(C) Representative gross picture showing the enlarged spleens present in the heterozygous nonubiquitinatable NEMO female mice relative to WT female littermate control mice. Flow-cytometry gating on the different subsets of splenic immune cells reveals that the percentage of $Gr_1^+CD11_b^+$ cells is greatly increased, suggesting an inflammatory phenotype in the heterozygous nonubiquitinatable NEMO mice.

The generation of TNFR1$^{-/-}$X^{NemoKi}Y mice also allowed us to determine the role that ubiquitination of NEMO plays in the NOD2 signaling pathway. Our previous biochemical mapping and signaling work was done in overexpression and reconstitution systems (Abbott et al., 2004, 2007), and the role that NEMO ubiquitination plays in NOD2 signaling in vivo has been unclear. The generation of this mouse allowed us to test the role of K285 and K399 ubiquitination in NOD2-driven innate immune signaling. To that end, we generated bone-marrow-derived macrophages (BMDMs) from WT, TNFR1$^{-/-}$, and TNFR1$^{-/-}$X^{NemoKi}Y mice

and treated them with the NOD2 agonist, MDP. Time courses showed that while p38 signaling was intact, MDP-induced NF-κB signaling and extracellular signal-regulated kinase (ERK) signaling were greatly diminished (Figure 5A). Because ERK signaling requires the IKKs to phosphorylate p105 (Yang et al., 2012), these features suggest a proximal defect at the level of the IKK signalosome. Importantly, NOD2 induction of NEMO ubiquitination was lost in the BMDMs derived from the TNFR1$^{-/-}$X^{NemoKi}Y mice (Figure 5B), whereas binding to the IKKs was retained (Figure S1). This suggests that the
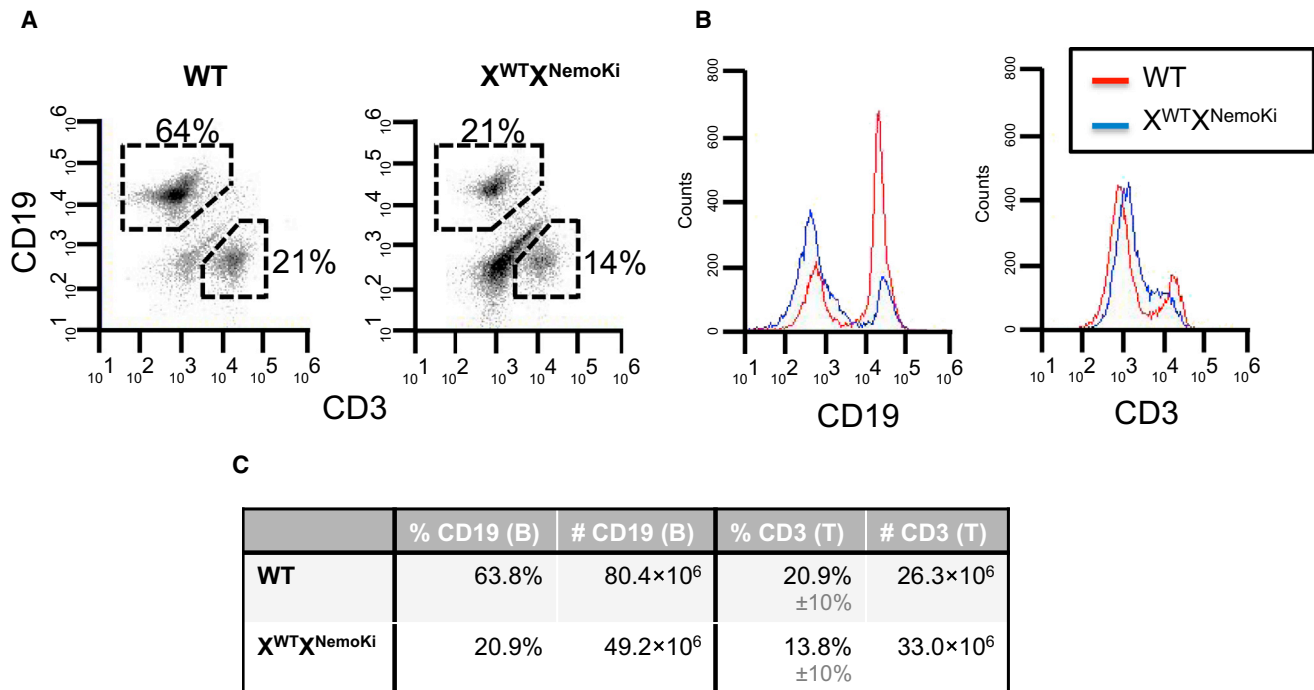
A

WT

64%

21%

CD19

CD3

X^WT^X^NemoKi^

21%

14%

B

Counts

CD19

Counts

CD3

WT
X^WT^X^NemoKi^

C

	% CD19 (B)	# CD19 (B)	% CD3 (T)	# CD3 (T)
WT	63.8%	80.4×10^6	20.9% ±10%	26.3×10^6
X^WT^X^NemoKi^	20.9%	49.2×10^6	13.8% ±10%	33.0×10^6

Figure 3. Normal T Cell Numbers but Decreased B Cell Numbers in the Spleens of X^WT^X^NemoKi^ Mice

(A) Flow cytometry with CD3 and CD19 antibodies shows that whereas CD19⁻CD3⁺ cells (T cells) are similar in number, C19⁺CD3⁻ (B cells) are greatly diminished in the X^WT^X^NemoKi^ mice.

(B) Graphical representation of the fluorescent intensity of CD19 and CD3 staining, again showing diminished B cells in the X^WT^X^NemoKi^ mice.

(C) Absolute number of splenic B and T cells in the WT and X^WT^X^NemoKi^ mice. Similar results were found in a total of three mice from each genotype.

replacement of these two lysine residues specifically affects ubiquitination but leaves the general folding of NEMO intact. To further verify this signaling defect, we performed qRT-PCR of genes induced by MDP in these BMDMs. In all cases, the TNFR1$^{-/-}$X^{NemoKi}Y BMDMs showed greatly decreased MDP-induced gene expression when stimulated by MDP (Figure 5C). In sum, these features suggest a broad defect in NOD2 signaling when NEMO cannot be ubiquitinated, and suggest that NEMO ubiquitination is central to NOD2 signaling.

To further determine the role that NEMO ubiquitination plays in generating and propagating innate immune signaling, we stimulated TNFR1$^{-/-}$X^{NemoKi}Y BMDMs with ultrapure LPS. Although the initial levels IκBα decreased similarly (see lanes 2 and 7 in Figure 6A), BMDMs from TNFR1$^{-/-}$X^{NemoKi}Y were not able to sustain an NF-κB response, as indicated by their inability to generate phosphorylated IκBα at later time points of stimulation (Figure 6A). This was recapitulated by a marked inability to generate LPS-driven cytokines (Figure 6B). Lastly, the ability of two additional innate immune stimuli to generate cytokine responses in these macrophages was determined. Limiting doses of IL-1 showed a defect in cytokine release (Figure 6C), whereas interferon γ (IFNγ) showed no specific defect (Figure 6D). This last point is an important control. Cytokine responses to IFNγ are dependent on JAK-STAT pathways and less so on NF-κB (Stark and Darnell, 2012). The fact that the IFNγ response is intact suggests that there is no broad immunologic signaling defect in these cells. Collectively, these find-

ings suggest that NEMO ubiquitination is crucial for NF-κB-directed cytokine responses.

DISCUSSION

Altogether, these findings highlight the importance of NEMO ubiquitination in NF-κB signaling. Genetically, NEMO ubiquitination is required for a functioning IKK signalosome, as evidenced by the fact that a NEMO allele that lacks the ability to be ubiquitinated at K285 and K399 largely phenocopies NEMO loss. Both NEMO null and NEMO K285RK399R mice show embryonic lethality due to TNF signaling, and in the female heterozygous state, both develop inflammatory skin lesions (Makris et al., 2000; Rudolph et al., 2000; Schmidt-Supprian et al., 2000). Thus, in addition to helping to coordinate NF-κB signaling through the binding of ubiquitinated proteins, NEMO itself must be ubiquitinated in order to function properly in the NF-κB pathway. Failure to do so causes not only embryonic lethality and steatohepatitis, but also dysfunction of a number of innate immune signaling systems.

Productive inflammation is important not only for the body to fight infection and damage, but also to avoid inflammatory disease. Because the NF-κB pathway represents one of the key inflammatory signaling pathways in the body, it is not surprising that there are numerous checks and balances to optimize signaling. One key point is that despite the fact that LPS-induced cytokine release is significantly compromised in the TNFR1$^{-/-}$X^{NemoKi}Y
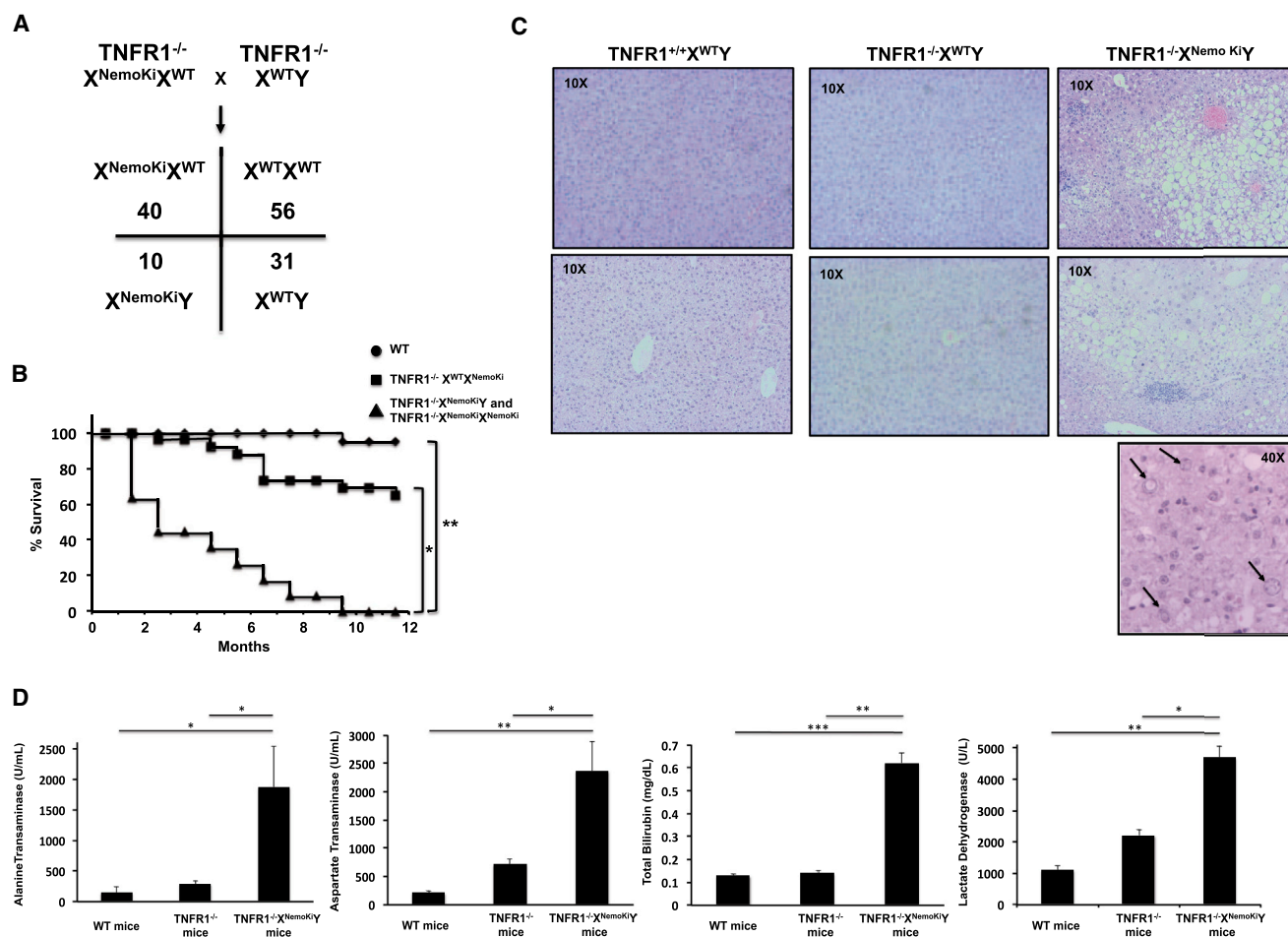
Figure 4. Mating onto a TNFR1-Deficient Background Rescues Embryonic Lethality in Nonubiquitinatable NEMO Mice, but Causes Steatohepatitis and Increased Mortality

(A) C57BL/6 TNFR1$^{-/-}$ mice were mated with TNFR1$^{+/+}$X^{WT}X^{NemoKi} mice and the resulting TNFR1$^{+/-}$X^{WT}X^{Nemoki} mice were mated with TNFR1$^{-/-}$X^{WT}Y mice to obtain TNFR1$^{-/-}$X^{WT}X^{NemoKi} mice, which were further mated with TNFR1$^{-/-}$X^{WT}Y to generate TNFR1$^{-/-}$X^{NemoKi}Y mice. The Mendelian ratios of this mating are shown. In a WT TNFR1 background, we did not obtain pure NEMO knockin mice; however, when TNFR1 was deleted, we obtained male nonubiquitinatable NEMO knockin mice, suggesting that TNFR1 deletion complements the nonubiquitinatable NEMO defect.

(B) Kaplan-Maier curves showing significantly decreased lifespans in the TNFR1$^{-/-}$X^{NemoKi}Y and TNFR1$^{-/-}$X^{NemoKi}X^{NemoKi} mice.

(C) Histologic evidence of steatohepatitis in the TNFR1$^{-/-}$X^{NemoKi}Y mice, including macro- and microvesicular steatosis, inflammatory infiltrates most prominent in zone 3 of the liver, and prominent nucleolar vacuolization (lower panel, nucleolar vacuolization is shown by arrows). These are all features of NASH.

(D) Elevated liver function tests in the TNFR1$^{-/-}$X^{NemoKi}Y mice, indicating significant hepatocyte injury. SEM, *p < 0.05, **p < 0.01, ***p < 0.001.

BMDMs, it is not completely abrogated. There is still a 10- to 20-fold increase in cytokine release in these BMDMs (Figure 6B). When compared with WT BMDMs, the increase is substantially lower; however, it is still measurable. The same is true for MDP and IL-1, albeit at a lower total induction level (Figures 5C and 6C). One interpretation of this finding is that the inability to induce site-specific NEMO ubiquitination is not absolutely required for signaling. It is only required for maximal signaling. Another interpretation, suggested by the equivalent initial decrease in IκBα levels upon LPS exposure with a failure to initiate a later wave of phosphorylation of IκBα (Figure 6A), is that NEMO ubiquitination might be required to sustain NF-κB signaling.

An additional area of interest lies in the fact that TNFR loss partially complements the NEMO knockin embryonic lethality.

The NEMO knockin females' fertility difficulties and irregular breeding precluded us from determining the cause of the embryonic lethality; however, the fact that mating onto a TNFR1$^{-/-}$ background complemented the lethality suggests that, like the NEMO null mice, the NEMO knockin mice die of TNF-induced liver apoptosis. This is interesting for two reasons. First, using reconstituted NEMO null MEFs, we previously showed that NEMO null cells reconstituted with K285R K399R NEMO via retroviral transfer show intact TNF signaling (Abbott et al., 2007). The differences between the in vitro system and the in vivo system could be due to developmental timing, cell-type specificity, or simple artifact due to overexpression. Second, the fact that TNFR1 loss complements the embryonic lethality suggests a genetic interaction. K399 ubiquitination was initially shown to
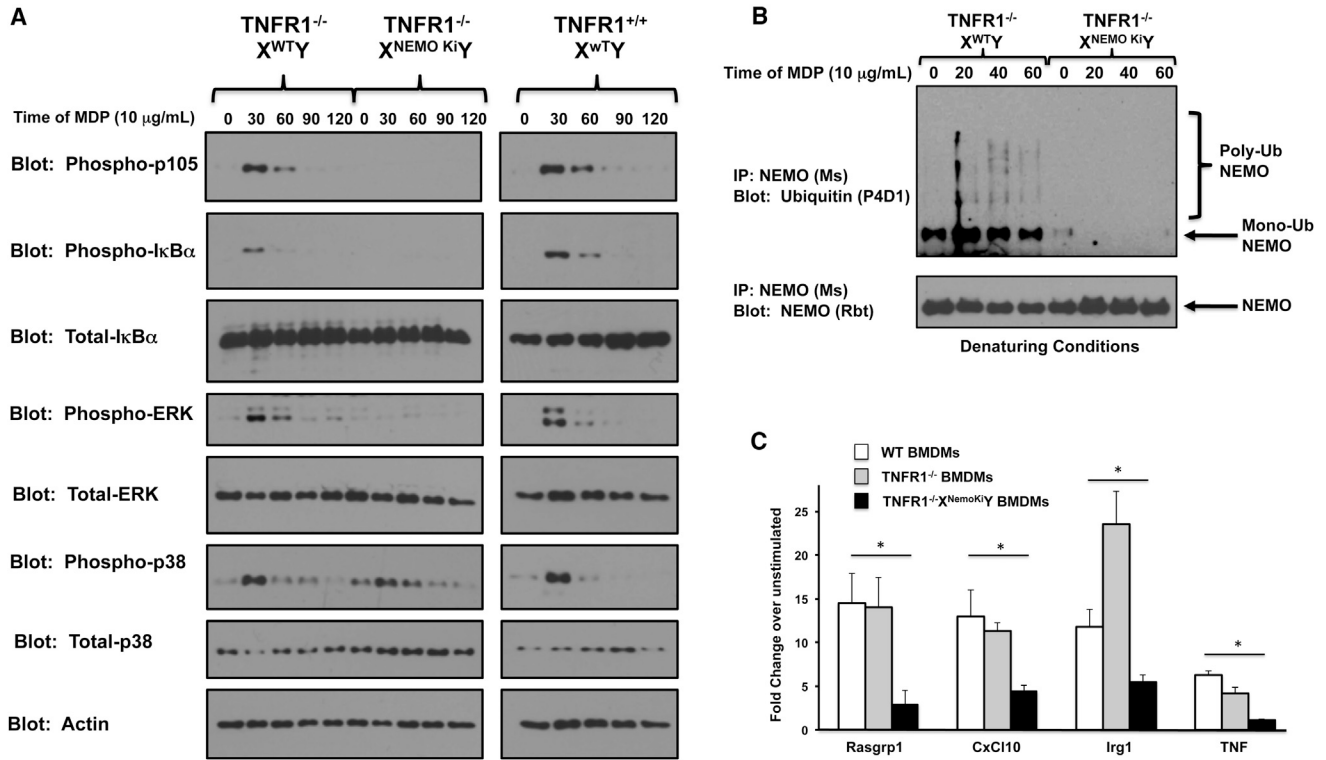
Figure 5. BMDMs Homozygous for Nonubiquitinatable NEMO Show a Severe Defect in NF-κB Signaling in Response to the NOD2 Agonist MDP

(A) Primary BMDMs were generated from TNFR1$^{-/-}$X^{WT}Y, TNFR1$^{-/-}$X^{NemoKi}Y, or TNFR1$^{+/+}$X^{WT}Y mice and were treated with 10 μg/ml of MDP for the indicated time period. BMDMs containing nonubiquitinatable NEMO showed an inability to phosphorylate two IKK substrates, IκBα and p105, in response to MDP. The inability to phosphorylate p105 further leads to an inability to activate p44/p42 ERK in response to MDP.

(B) Primary BMDMs were generated from TNFR1$^{-/-}$X^{WT}Y or TNFR1$^{-/-}$X^{NemoKi}Y mice and were treated with 10 μg/ml of MDP for the indicated time period. Lysates were generated in denaturing conditions (boiled with 1% SDS). After cooling, the SDS was diluted to 0.1% and NEMO immunoprecipitation was performed. Western blotting showed that although WT NEMO could be inducibly ubiquitinated, knockin NEMO could not.

(C) To quantitate the signaling effect and to determine the role of NEMO ubiquitination in MDP-induced gene expression, the indicated BMDMs were treated with 10 mg/ml MDP for 4 hr before RNA was harvested and subjected to qRT-PCR. In all cases studied, the BMDMs expressing nonubiquitinatable NEMO showed greatly decreased MDP-induced gene expression. SEM, *p < 0.05, **p < 0.01, ***p < 0.001.

be TNF inducible by mutagenesis and reconstitution studies, and was further shown to be required for optimal TNF-induced NF-κB activity in tissue culture systems (Zhou et al., 2004). In contrast, despite the fact that K285 has been shown repeatedly to be directly ubiquitinated in mass spectrometry experiments by numerous groups (Abbott et al., 2004; Hinz et al., 2010; Kim et al., 2011; Niu et al., 2011), K285 ubiquitination has not yet been linked in vivo to TNF signaling. Although a K285R-only mouse has not been generated, the fact that the described K399R (K391R mouse) does not show embryonic lethality, coupled with the fact that the K285RK399R knockin mouse's embryonic lethality can be complemented by TNFR1 loss, implies that K285 ubiquitination may be required for optimal TNF family member signaling. Future work will address this possibility both genetically and biochemically.

In summary, while ubiquitin chain binding by NEMO has been shown to be important in physiologic NF-κB signaling, this work shows that site-specific ubiquitination of NEMO is required for physiologic NF-κB signaling as well.

EXPERIMENTAL PROCEDURES

Generation of NEMO Knockin Mice

NEMO knockin mice were generated under contract by Ingenious Targeting Labs. The targeting vector shown in Figure 1A was designed to knock a cDNA containing a full-length myc-tagged NEMO containing K285R and K399R into exons 2–5 of the endogenous NEMO allele. After electroporation into embryonic stem cells (ESCs; BA1 hybrid 129svev/C57Bl6N) and generation of stably integrated clones, as evidenced by both PCR and Southern blotting, the ESCs were injected into C57Bl/6 blastocysts. Ten chimeric mice (six males and four females) were derived. All six of the males showed 80%–90% chimerism and two of the females showed 80%–90% chimerism. The chimeric mice were mated and germline transmission of the knocked-in Nemo gene was confirmed by PCR. These mice were twice backcrossed onto C57BL/6 FLT mice to excise the NEO cassette, and were further backcrossed onto C57BL/6 eight additional times before experiments were performed. TNFR1−/− mice were obtained from The Jackson Laboratory.

Antibodies, Reagents, and Chemicals

Myc, NEMO (rbt), IKKα, IKKβ, pIκBα, IκBα, phospho-ERK, ERK, phospho-p105, phospho-p38, and p38 were obtained from Cell Signaling Technologies. Anti-Actin was obtained from Santa Cruz Biotechnologies. Anti-NEMO
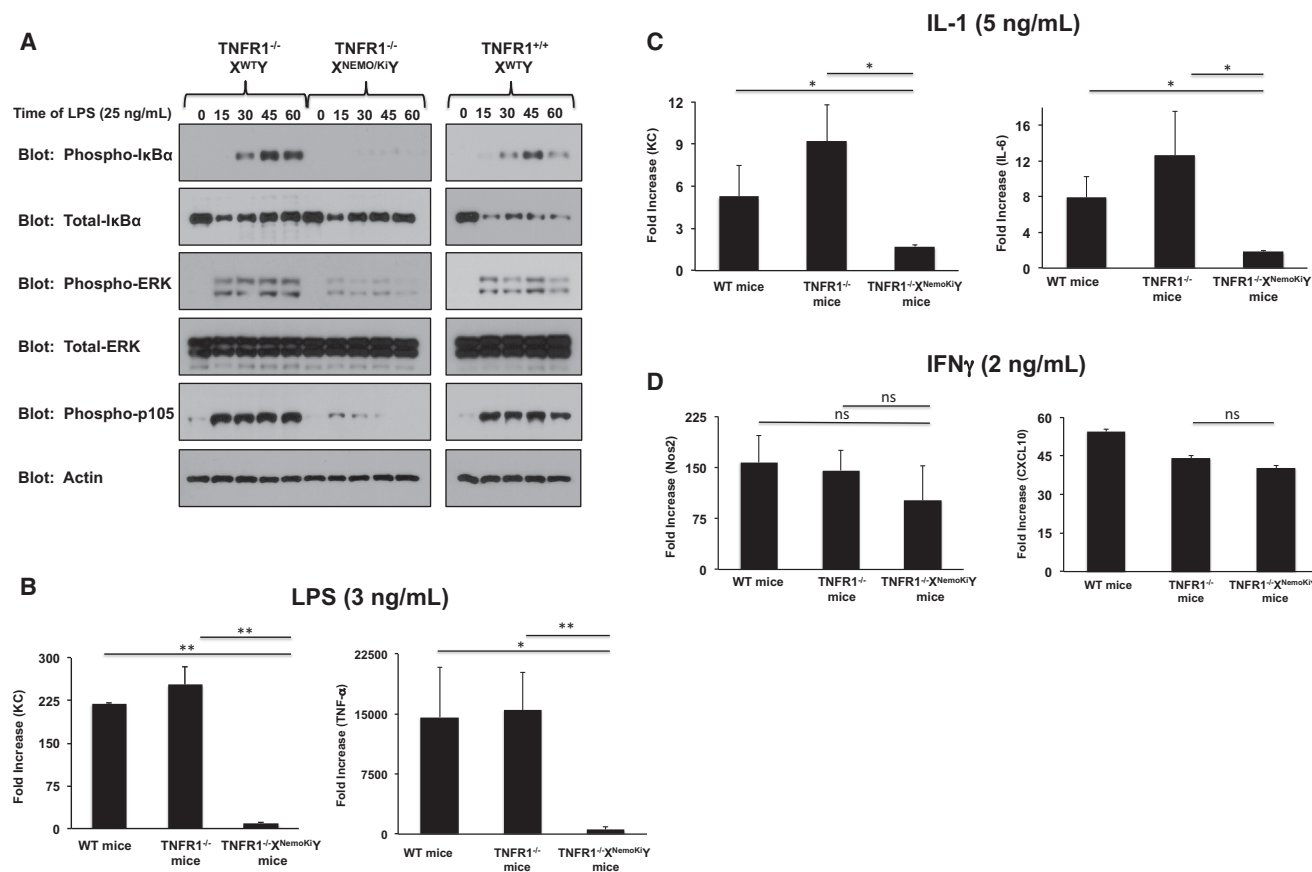
Figure 6. BMDMs Homozygous for Nonubiquitinatable NEMO Show Defects in TLR4 and IL-1 Responses but Normal IFN Responses

(A) Primary BMDMs were generated from TNFR1$^{-/-}$X^{WT}Y, TNFR1$^{-/-}$X^{NemoKi}Y, or TNFR1$^{+/+}$X^{WT}Y mice and were treated with 25 ng/ml of LPS for the indicated time period. Although the initial levels of total IκBα dropped in all three genetic lines, only BMDMs with WT NEMO could sustain an NF-κB response, as indicated by phospho-IκBα and phospho-p105 blots. Erk signaling was likewise substantially diminished.

(B) To quantify and verify these signaling results, the indicated BMDMs were treated with LPS (3 ng/ml) for 4 hr. RNA was harvested and subjected to qRT-PCR. Although all three genetic lines showed an increase in KC or TNF-α production, this was severely decreased in the BMDMs from TNFR1$^{-/-}$X^{NemoKi}Y mice. SEM, *p < 0.05, **p < 0.01.

(C) The indicated BMDMs were treated with IL-1 (5 ng/ml) for 4 hr before cells were harvested and subjected to qRT-PCR. IL-1-induced KC and IL-6 expression was significantly impaired in the TNFR1$^{-/-}$X^{NemoKi}Y BMDMs. SEM, *p < 0.05.

(D) The indicated BMDMs were treated with IFN-γ (2 ng/ml) for 4 hr before cells were harvested and subjected to qRT-PCR. There were no significant changes in gene expression between any of the cell lines. SEM.

(monoclonal mouse clone C73-764) was obtained from BD Biosciences. MDP was obtained from Bachem. Ultrapure LPS was obtained from InvivoGen. IL-1 was obtained from R&D Systems. All antibodies used in flow cytometry were obtained from BioLegend.

BMDM Generation, Western Blotting, and Liver Function Tests

BMDMs from age- and sex-matched mice were generated by culturing BM from the indicated mice for 7 days in 10% Dulbecco's modified Eagle's medium (DMEM) with 25% conditioned Ladmac medium (a gift from Clifford Harding, CWRU). The medium was changed to 10% fetal bovine serum (FBS)-DMEM overnight before use. Western blotting was performed as previously described. Liver function tests were performed on whole blood at the Mouse Physiology Core Facility of UC Davis.

Flow Cytometry

Spleens were harvested from mice 2 months of age. For each experiment, age- and sex-matched mice were used. Splenocytes were resuspended in RPMI with 10% serum and passed through a 70 μm cell strainer before centri-

fugation at 1,200 rpm for 5 min. Red blood cells were lysed and cells were adjusted to a concentration of 20 × 10^6 cells/ml; 50 μl of cells (1 × 10^6 cells) were used for each staining condition. FcBlock was diluted according to the recommended concentration and 25 μl was added to the cells for 5 min on ice to block nonspecific binding. FcBlock, FITC anti-CD11b, APC anti-Gr1, PE anti-CD11c, FITC anti-CD3, PE anti-CD19, FITC anti-CD4, PE anti-CD8, and PE anti-Ly6G were all obtained from eBioscience. Antibody cocktails were made fresh for each staining condition and 25 μl of cocktail was added to the cells (for a total staining volume of 100 μl). Cells were stained for 1 hr on ice, washed twice with PBS, and resuspended in 300 μl PBS. Data were acquired using an A6 Accuri Flow cytometer (Invitrogen) and analyzed using CFlow software (Invitrogen).

qRT-PCR and Statistical Analysis

RNA was isolated and reverse transcribed using a Quantitect RT kit (QIAGEN). Primer sequences are listed in Tigno-Aranjuez et al. (2010). Sybr green was obtained from Bio-Rad, and real-time PCRs were carried out with a CFX96 C1000 Real-Time Thermal Cycler from Bio-Rad. RT-PCR data are presented as the

mean ± SEM. RT-PCR experiments were performed in duplicate and repeated twice. Results of representative experiments are shown. The significance of the comparisons shown was assessed by Student's two-tailed t test or a chi-square test with the cutoff for significance set at $p \leq 0.05$.

SUPPLEMENTAL INFORMATION

Supplemental Information includes one figure and can be found with this article online at http://dx.doi.org/10.1016/j.celrep.2013.06.036.

REFERENCES

Abbott, D.W., Wilkins, A., Asara, J.M., and Cantley, L.C. (2004). The Crohn's disease gene, NOD2, requires RIP2 in order to induce ubiquitinylation of a novel site on NEMO. Curr. Biol. *14*, 2217–2227.

Abbott, D.W., Yang, Y., Hutti, J.E., Madhavarapu, S., Kelliher, M.A., and Cantley, L.C. (2007). Coordinated regulation of Toll-like receptor and NOD2 signaling by K63-linked polyubiquitin chains. Mol. Cell. Biol. *27*, 6012–6025.

Belgnaoui, S.M., Paz, S., Samuel, S., Goulet, M.L., Sun, Q., Kikkert, M., Iwai, K., Dikic, I., Hiscott, J., and Lin, R. (2012). Linear ubiquitination of NEMO negatively regulates the interferon antiviral response through disruption of the MAVS-TRAF3 complex. Cell Host Microbe *12*, 211–222.

Beraza, N., Lüdde, T., Assmus, U., Roskams, T., Vander Borght, S., and Trautwein, C. (2007). Hepatocyte-specific IKK gamma/NEMO expression determines the degree of liver injury. Gastroenterology *132*, 2504–2517.

Beraza, N., Malato, Y., Sander, L.E., Al-Masaoudi, M., Freimuth, J., Riethmacher, D., Gores, G.J., Roskams, T., Liedtke, C., and Trautwein, C. (2009). Hepatocyte-specific NEMO deletion promotes NK/NKT cell- and TRAIL-dependent liver damage. J. Exp. Med. *206*, 1727–1737.

Chen, Z.J. (2012). Ubiquitination in signaling to and activation of IKK. Immunol. Rev. *246*, 95–106.

Chen, G., Shaw, M.H., Kim, Y.G., and Nuñez, G. (2009). NOD-like receptors: role in innate immunity and inflammatory disease. Annu. Rev. Pathol. *4*, 365–398.

Cordier, F., Grubisha, O., Traincard, F., Véron, M., Delepierre, M., and Agou, F. (2009). The zinc finger of NEMO is a functional ubiquitin-binding domain. J. Biol. Chem. *284*, 2902–2907.

Derudder, E., Cadera, E.J., Vahl, J.C., Wang, J., Fox, C.J., Zha, S., van Loo, G., Pasparakis, M., Schlissel, M.S., Schmidt-Supprian, M., and Rajewsky, K. (2009). Development of immunoglobulin lambda-chain-positive B cells, but not editing of immunoglobulin kappa-chain, depends on NF-kappaB signals. Nat. Immunol. *10*, 647–654.

Girardin, S.E., Boneca, I.G., Viala, J., Chamaillard, M., Labigne, A., Thomas, G., Philpott, D.J., and Sansonetti, P.J. (2003). Nod2 is a general sensor of peptidoglycan through muramyl dipeptide (MDP) detection. J. Biol. Chem. *278*, 8869–8872.

Hadian, K., Griesbach, R.A., Dornauer, S., Wanger, T.M., Nagel, D., Metlitzky, M., Beisker, W., Schmidt-Supprian, M., and Krappmann, D. (2011). NF-κB essential modulator (NEMO) interaction with linear and lys-63 ubiquitin chains contributes to NF-κB activation. J. Biol. Chem. *286*, 26107–26117.

Hayden, M.S., and Ghosh, S. (2012). NF-κB, the first quarter-century: remarkable progress and outstanding questions. Genes Dev. *26*, 203–234.

Hinz, M., Stilmann, M., Arslan, S.C., Khanna, K.K., Dittmar, G., and Scheidereit, C. (2010). A cytoplasmic ATM-TRAF6-cIAP1 module links nuclear DNA damage signaling to ubiquitin-mediated NF-κB activation. Mol. Cell *40*, 63–74.

Ikeda, F., Rahighi, S., Wakatsuki, S., and Dikic, I. (2011). Selective binding of linear ubiquitin chains to NEMO in NF-kappaB activation. Adv. Exp. Med. Biol. *691*, 107–114.

Inohara, N., Ogura, Y., Fontalba, A., Gutierrez, O., Pons, F., Crespo, J., Fukase, K., Inamura, S., Kusumoto, S., Hashimoto, M., et al. (2003). Host recognition of bacterial muramyl dipeptide mediated through NOD2. Implications for Crohn's disease. J. Biol. Chem. *278*, 5509–5512.

Kensche, T., Tokunaga, F., Ikeda, F., Goto, E., Iwai, K., and Dikic, I. (2012). Analysis of nuclear factor-κB (NF-κB) essential modulator (NEMO) binding to linear and lysine-linked ubiquitin chains and its role in the activation of NF-κB. J. Biol. Chem. *287*, 23626–23634.

Kim, S., La Motte-Mohs, R.N., Rudolph, D., Zuniga-Pflucker, J.C., and Mak, T.W. (2003). The role of NF-kB essential modulator (NEMO) in B cell development and survival. Proc. Natl. Acad. Sci. USA *100*, 1203–1208.

Kim, W., Bennett, E.J., Huttlin, E.L., Guo, A., Li, J., Possemato, A., Sowa, M.E., Rad, R., Rush, J., Comb, M.J., et al. (2011). Systematic and quantitative assessment of the ubiquitin-modified proteome. Mol. Cell *44*, 325–340.

Laplantine, E., Fontan, E., Chiaravalli, J., Lopez, T., Lakisic, G., Véron, M., Agou, F., and Israël, A. (2009). NEMO specifically recognizes K63-linked poly-ubiquitin chains through a new bipartite ubiquitin-binding domain. EMBO J. *28*, 2885–2895.

Lo, Y.C., Lin, S.C., Rospigliosi, C.C., Conze, D.B., Wu, C.J., Ashwell, J.D., Eliezer, D., and Wu, H. (2009). Structural basis for recognition of diubiquitins by NEMO. Mol. Cell *33*, 602–615.

Luedde, T., Beraza, N., Kotsikoris, V., van Loo, G., Nenci, A., De Vos, R., Roskams, T., Trautwein, C., and Pasparakis, M. (2007). Deletion of NEMO/IKKgamma in liver parenchymal cells causes steatohepatitis and hepatocellular carcinoma. Cancer Cell *11*, 119–132.

Makris, C., Godfrey, V.L., Krähn-Senftleben, G., Takahashi, T., Roberts, J.L., Schwarz, T., Feng, L., Johnson, R.S., and Karin, M. (2000). Female mice heterozygous for IKK gamma/NEMO deficiencies develop a dermatopathy similar to the human X-linked disorder incontinentia pigmenti. Mol. Cell *5*, 969–979.

Nenci, A., Huth, M., Funteh, A., Schmidt-Supprian, M., Bloch, W., Metzger, D., Chambon, P., Rajewsky, K., Krieg, T., Haase, I., and Pasparakis, M. (2006). Skin lesion development in a mouse model of incontinentia pigmenti is triggered by NEMO deficiency in epidermal keratinocytes and requires TNF signaling. Hum. Mol. Genet. *15*, 531–542.

Ni, C.Y., Wu, Z.H., Florence, W.C., Parekh, V.V., Arrate, M.P., Pierce, S., Schweitzer, B., Van Kaer, L., Joyce, S., Miyamoto, S., et al. (2008). Cutting edge: K63-linked polyubiquitination of NEMO modulates TLR signaling and inflammation in vivo. J. Immunol. *180*, 7107–7111.

Niu, J., Shi, Y., Iwai, K., and Wu, Z.H. (2011). LUBAC regulates NF-κB activation upon genotoxic stress by promoting linear ubiquitination of NEMO. EMBO J. *30*, 3741–3753.

Rahighi, S., Ikeda, F., Kawasaki, M., Akutsu, M., Suzuki, N., Kato, R., Kensche, T., Uejima, T., Bloor, S., Komander, D., et al. (2009). Specific recognition of linear ubiquitin chains by NEMO is important for NF-kappaB activation. Cell *136*, 1098–1109.

Rudolph, D., Yeh, W.-C., Wakeham, A., Rudolph, B., Nallainathan, D., Potter, J., Elia, A.J., and Mak, T.W. (2000). Severe liver degeneration and lack of NF-kappaB activation in NEMO/IKKgamma-deficient mice. Genes Dev. *14*, 854–862.

Schmidt-Supprian, M., Bloch, W., Courtois, G., Addicks, K., Israël, A., Rajewsky, K., and Pasparakis, M. (2000). NEMO/IKK gamma-deficient mice model incontinentia pigmenti. Mol. Cell *5*, 981–992.

Stark, G.R., and Darnell, J.E., Jr. (2012). The JAK-STAT pathway at twenty. Immunity *36*, 503–514.

Tigno-Aranjuez, J.T., Asara, J.M., and Abbott, D.W. (2010). Inhibition of RIP2's tyrosine kinase activity limits NOD2-driven cytokine responses. Genes Dev. *24*, 2666–2677.

Tokunaga, F., Sakata, S., Saeki, Y., Satomi, Y., Kirisako, T., Kamei, K., Nakagawa, T., Kato, M., Murata, S., Yamaoka, S., et al. (2009). Involvement of linear polyubiquitylation of NEMO in NF-kappaB activation. Nat. Cell Biol. *11*, 123–132.

Wu, C.J., Conze, D.B., Li, T., Srinivasula, S.M., and Ashwell, J.D. (2006). Sensing of Lys 63-linked polyubiquitination by NEMO is a key event in NF-kappaB activation [corrected]. Nat. Cell Biol. *8*, 398–406.

Yang, H.T., Papoutsopoulou, S., Belich, M., Brender, C., Janzen, J., Gantke, T., Handley, M., and Ley, S.C. (2012). Coordinate regulation of TPL-2 and NF-κB signaling in macrophages by NF-κB1 p105. Mol. Cell. Biol. *32*, 3438–3451.

Zhao, T., Yang, L., Sun, Q., Arguello, M., Ballard, D.W., Hiscott, J., and Lin, R. (2007). The NEMO adaptor bridges the nuclear factor-kappaB and interferon regulatory factor signaling pathways. Nat. Immunol. *8*, 592–600.

Zhou, H., Wertz, I., O'Rourke, K., Ultsch, M., Seshagiri, S., Eby, M., Xiao, W., and Dixit, V.M. (2004). Bcl10 activates the NF-kappaB pathway through ubiquitination of NEMO. Nature *427*, 167–171.
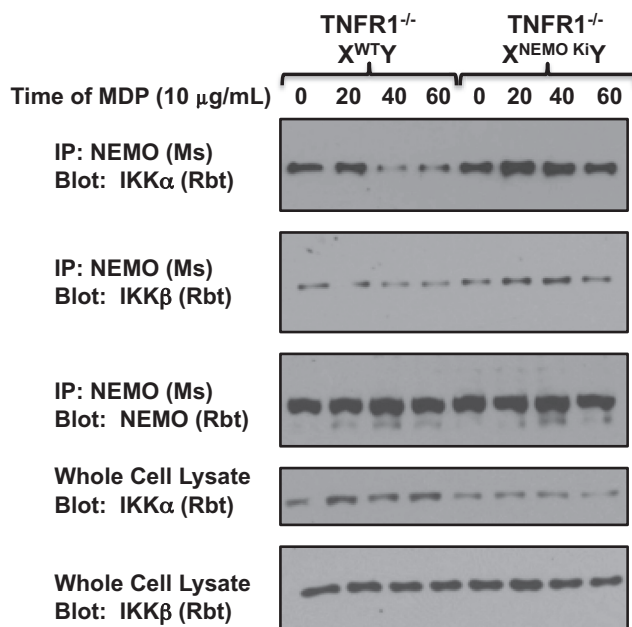
Figure S1. NemoKi Can Bind to IKKs, Related to Results

BMDMs from TNFR1$^{-/-}$X^{WT}Y or TNFR1$^{-/-}$X^{NemoKi}Y mice were treated with 10 μg/ml MDP for the indicated time period. Cells were then harvested in lysis buffer and immunoprecipitated with an anti-NEMO monoclonal antibody. Western blotting showed that NEMO bound the IKKs, suggesting that at least the N-terminal region of NEMO (IKK interaction domain) was properly folded.